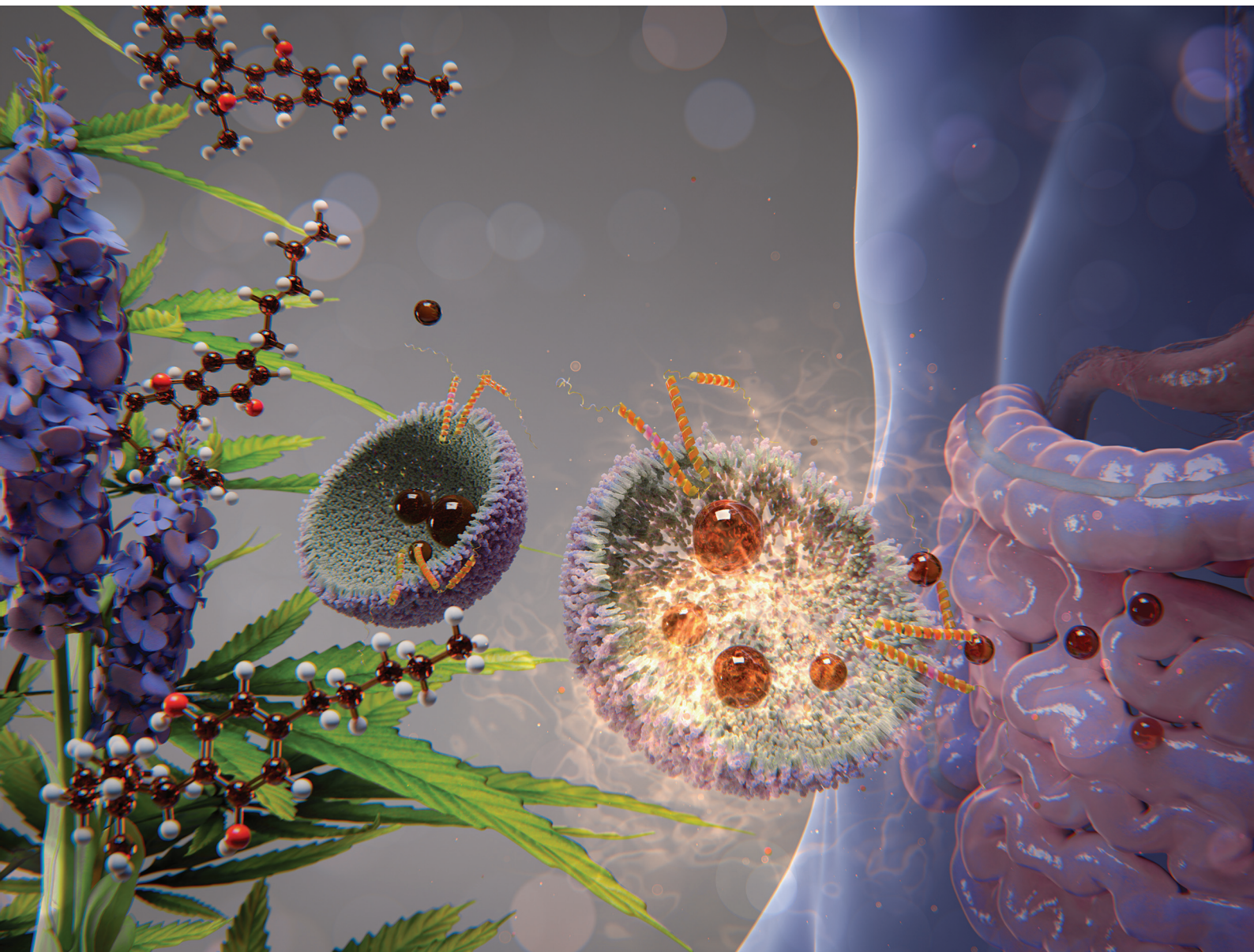


# Food & Function

Linking the chemistry and physics of food with health and nutrition

[rsc.li/food-function](http://rsc.li/food-function)



ISSN 2042-650X



Cite this: *Food Funct.*, 2025, **16**, 6369

## Controlled *in vitro* release of CBD from oleosomes via modulation of their membrane density†

Zhaoliang Ma,<sup>a,b</sup> Edoardo Capuano,<sup>ID c</sup> Johannes H. Bitter,<sup>ID a</sup> Remko M. Boom<sup>b</sup> and Constantinos V. Nikiforidis <sup>ID \*a</sup>

Oleosomes, native lipid droplets abundant in the plant kingdom, especially in oilseeds, can be extracted in simple steps and have been suggested as lipid carriers or natural substitutes for oil droplets in emulsion-like products for foods, cosmetics and pharmaceuticals. Oleosomes are good candidates as lipid carriers via the oral route due to their limited hydrolysis during gastric digestion and slow hydrolysis in the small intestinal phase. The factors that affect oleosomes' ability to resist *in vitro* digestion, particularly the influence of their membrane molecular composition and density, remain unknown. Therefore, oleosome lipid hydrolysis was investigated in a model of small intestinal digestion and compared with oil droplets stabilized by whey proteins and/or phospholipids and with oleosomes having lower membrane density. To showcase that the lipid hydrolysis rate can also affect cargo release, oleosomes were loaded with cannabidiol (CBD) and the CBD release was tracked. Oleosomes exhibited significantly slower lipid digestion than the droplets stabilised by whey proteins and/or phospholipids, which were rapidly digested. The low lipid hydrolysis of oleosomes during intestinal digestion has been attributed to the unique structure of the oleosome membrane proteins, oleosins, which have a long amphipathic helix pinned into the oleosome oil core and out of reach for bile salts and enzymes. Oleosomes with lower membrane density exhibited faster lipid hydrolysis, probably because the digestive enzymes could better adsorb on the interface to access the core lipids. The results elucidate the factors that affect the lipid digestion of oleosomes and demonstrate the dynamic nature of oleosomes for the controlled release of lipophilic cargos, such as CBD, in the intestinal tract.

Received 3rd September 2024,  
Accepted 12th May 2025

DOI: 10.1039/d4fo04171b  
[rsc.li/food-function](http://rsc.li/food-function)

## 1. Introduction

The development of carriers for the targeted delivery of bioactive molecules has gained significant attention in recent years, particularly for applications within the gastrointestinal tract. The main drawbacks of the currently used carriers are the *in vivo* cytotoxicity combined with their low absolute loading capacity.<sup>1,2</sup> There is increased interest in further developing this field with more biobased and biocompatible solutions to overcome these issues.<sup>3,4</sup>

Oleosomes, also known as lipid droplets, constitute a potential natural carrier for transporting hydrophobic functional ingredients. They are abundant in oilseeds and can be

isolated by simple aqueous extraction without the need for chemical- or energy-intensive procedures.<sup>5,6</sup> Oleosomes are physically stable droplets with a diameter of around 0.2–2.0 µm equipped with a protective monolayer of phospholipids and a unique family of proteins named oleosins.<sup>7</sup> Oleosins have a hairpin structure consisting of two short, mobile hydrophilic flanks on the membrane, while their characteristic amphipathic helix is inserted in the lipid core.<sup>6</sup> The oleosome membrane structure is permeable to lipophilic molecules, such as curcumin and cannabidiol (CBD),<sup>8,9</sup> which can be encapsulated into oleosomes and potentially delivered through oral administration. Using oleosomes for the oral delivery of lipophilic cargoes is promising since it has been demonstrated that oleosomes may be slowly digested in *in vitro* models of digestion.<sup>10,11</sup> Besides the efficient delivery of cargo to the intestine, a slower FFA release and a potential lower lipid digestibility are positive for issues associated with a fast increase in post-prandial triglyceride levels in the blood.<sup>12</sup> There is currently no clear insight into the exact role of the oleosome membrane on lipid digestion rates. Some studies have indicated that heating can alter the structure of the oleosome membrane, leading to the enhancement of lipid

<sup>a</sup>Biobased Chemistry and Technology, Wageningen University and Research, Bornse Weilanden 9, PO Box 17, 6708 WG Wageningen, The Netherlands

<sup>b</sup>Food Process Engineering, Wageningen University and Research, Bornse Weilanden 9, PO Box 17, 6708 WG Wageningen, The Netherlands

<sup>c</sup>Food Quality and Design, Wageningen University and Research, Bornse Weilanden 9, PO Box 17, 6708 WG Wageningen, The Netherlands

† Electronic supplementary information (ESI) available. See DOI: <https://doi.org/10.1039/d4fo04171b>



digestion.<sup>13,14</sup> However, the effect of the membrane molecules and their packing on the lipid digestion rate is still a research area that requires further exploration.

The present study aims to understand the (*in vitro*) digestibility of hemp seed oleosomes loaded with CBD by modulating the membrane density and also comparing it to oil droplets stabilised by whey proteins and phospholipids.

CBD is a hydrophobic and non-psychoactive cannabinoid associated with many therapeutic benefits.<sup>15</sup> CBD is unstable in physiological conditions, exhibiting poor bioavailability,<sup>16</sup> making it an appropriate model molecule for a proof-of-concept controlled delivery using oleosomes.

## 2. Materials and methods

### 2.1 Materials

Hemp seeds were provided by Botaneco Inc. (Calgary, Canada). Whey protein isolate (WPI) was purchased from Davisco Foods International (BiPro, Eden Prairie, Minnesota, USA; purity 97.5%). Phospholipids (PL) were purchased from Avanti Polar Lipids, Inc. (Alabaster, AL, USA). CBD was purchased from Rocky Mountain High (Vail, USA). Ethanol and acetonitrile (ACN) were obtained from Actu-All Chemicals B.V. (Oss, The Netherlands). Pepsin from porcine gastric mucosa (P7000,  $\geq 250$  units per mg), lipase from porcine pancreas (L3126,  $\geq 125$  units per mg), porcine bile extract (B8631) and all other analytical grade chemicals used in this work were purchased from Sigma Aldrich (St. Louis, MO, USA). Milli-Q water was used to prepare all solutions unless specified otherwise.

### 2.2 Hemp seed oleosome extraction

Hemp seed oleosomes were extracted using an aqueous extraction procedure.<sup>5</sup> Hemp seeds were soaked in Milli-Q water at a ratio of 1 : 7 (w/w) at pH 8.0 adjusted with 1.0 M NaOH and stored at 4 °C overnight in a fridge. The soaked hemp seeds were re-adjusted to pH 8.0 and blended in a laboratory blender (8010ES, Waring Product Division, New Hartford, CT, USA) for 60 s. Cheesecloth was used to remove all the residues from the slurry. The filtrate was adjusted to pH 8.0 and centrifuged (4000g) at 4 °C for 30 min. The top cream layer was collected and fully redispersed in Milli-Q water of pH 8.0 (1 : 9, w/w) and centrifuged at 10 000g for 30 min at 4 °C. After the centrifugation, hemp seed oleosomes were collected, and excess water was removed.

### 2.3 CBD encapsulation into oleosomes

Purified hemp seed oleosomes were dispersed into Milli-Q water at a ratio of 1 : 9 (w/w) to prepare oleosome dispersions with 10 wt% oil. CBD was encapsulated into the fresh oleosome dispersions using the co-solvent method.<sup>8</sup> CBD was initially dissolved in ethanol and then added to the fresh oleosome dispersions with the final concentrations of CBD at 0.1 wt%, ethanol at 7.5 wt% and oil at 7.5 wt%. The mixtures were stirred at 200 rpm for 10 min at 20 °C. After encapsulation, the mixtures were centrifuged at 5000g for 15 min at 4 °C

to separate the cream layer with the encapsulated CBD and to remove the unencapsulated CBD at the bottom. The obtained CBD-loaded oleosomes were collected and dispersed again in Milli-Q water as CBD-loaded oleosome dispersions (7.5 wt% oil content).

The encapsulation efficiency of CBD (EE) in samples was analyzed using the method described in section 2.7 and calculated according to eqn (1), as follows:

$$\text{Encapsulation efficiency, EE (\%)} = \frac{C_0}{C_{\text{Initial}}} \times 100\% \quad (1)$$

where  $C_0$  is the concentration of CBD encapsulated in CBD-loaded oleosomes, and  $C_{\text{Initial}}$  is the CBD concentration initially added.

### 2.4 Treatments on oleosomes

**2.4.1 Preparation of heat-treated oleosomes.** The freshly prepared oleosome dispersions (7.5 wt% oil content) were heated at 95 °C for 30 min in a water bath. After heating, samples were immediately cooled to room temperature by immersion in an ice bath (7.5 wt% oil content).

**2.4.2 Homogenization of oleosomes with additional hemp seed oil.** The freshly prepared oleosome dispersions (3.75 wt% oil content) were homogenized with an equivalent mass of additional hemp seed oil (3.75 wt%) by passing through a high-pressure homogenizer (GEA, Niro Soavi NS 1001 L, Parma, Italy) at a pressure of 250 bars for 5 passes to obtain homogenized oleosomes (7.5 wt% oil content).

### 2.5 Protein profile characterization

The protein profiles of heated and unheated oleosomes were analyzed using SDS-PAGE.<sup>5</sup> Every oleosome dispersion sample (100  $\mu$ L) was mixed with 650  $\mu$ L of Milli-Q water and 250  $\mu$ L of sample buffer and centrifuged for 1 min at 2000 rpm. The centrifuged mixtures were heated at 70 °C for 10 min and centrifuged again. Then, 20  $\mu$ L of the obtained samples was loaded on the 4–12% Bis-Tris gel. The protein marker had a molecular weight of 10–250 kDa. Electrophoresis was executed for 30 min at 200 V. The gel was stained with Coomassie Brilliant Blue R-250 staining solution.

### 2.6 Formulation of oil-in-water emulsions with whey proteins and/or phospholipids

The surfactant concentrations were selected based on the natural levels of interfacial molecules in oleosomes. Previous analyses indicated that the content of lipids (75 wt%) and proteins (6 wt%) in purified hemp seed oleosomes could be used as a reference.<sup>5</sup> The literature also suggests that hemp seed oleosomes contain  $206 \pm 7$  mg of phospholipids per 100 g of lipids (0.21 wt%).<sup>17</sup> To obtain a stable emulsion system, three different continuous phases were prepared, containing whey protein isolate (WPI) 1.0 wt%, phospholipids (PL) 1.0 wt%, and both WPI (1.0 wt%) and PL (1.0 wt%), WPI + PL, by dissolution in MilliQ-water and stirring overnight at room temperature, respectively. Hemp seed oil was prepared by dissolving 0.1 wt% CBD as the dispersed phase. The CBD-loaded oil-in-



water (O/W) emulsions were prepared by homogenizing 7.5 wt% dispersed phase with 92.5 wt% continuous phase at room temperature *via* a two-step homogenization procedure. The coarse emulsions were prepared by homogenizing the two phases at 8000 rpm for 5 min in an IKA (Ultra-Turrax, IKA, Staufen, Germany) and then passed through a high-pressure homogenizer (GEA, Niro Soavi NS 1001 L, Parma, Italy) at a pressure of 30 bars for 5 passes to obtain fine emulsions.

## 2.7 Quantification of CBD

CBD was extracted from the CBD-loaded oleosomes by solvent extraction. CBD-loaded oleosome dispersions or CBD-loaded emulsions (200  $\mu$ L) were diluted in a 10 mL volumetric flask with ACN to extract the CBD from samples and then transferred to HPLC vials by passing through a syringe filter (pore size 0.2  $\mu$ m). The CBD content was quantified with an UltiMate 3000 UHPLC system (ThermoFisher Scientific). The filtered solution (10  $\mu$ L) was injected into the UHPLC system equipped with an Acquity UPLC BEH C18 column (150 mm  $\times$  2.1 mm, 1.7  $\mu$ m particle size, Waters, Massachusetts, US) and a UV-vis spectrophotometric detector. Milli-Q water and ACN were prepared as mobile phases A and B, respectively. The mobile phase flow rate was set at 0.38 mL min $^{-1}$  with a column temperature of 35 °C. The mobile phase gradient conditions were set as follows: 0–1 min, kept at 50% B; 1–10 min, increased from 50% to 100% B; 10–15 min, kept at 100% B; 15–20 min, kept at 50% B. The detection wavelength was set at 220 nm.

## 2.8 Droplet size distribution

A Bettersizer S3 Plus (Bettersize Instruments Ltd, China) static light diffraction system was used to measure the droplet size ( $d_{4,3}$ ) and size distribution of oleosomes and different types of oil droplets (1 mL) mixed with the same volume of 1.0 wt% SDS solution which could break the aggregation between droplets produced by the bridging of proteins on the surface of oleosomes. The refractive indices of continuous and dispersed phases were set at 1.33 and 1.47, respectively.

## 2.9 *In vitro* digestion of oleosomes and bioaccessibility of CBD

The *in vitro* digestion of oleosomes was investigated using a gastrointestinal (GIT) model, which included both the gastric and the intestinal phases.<sup>11,18</sup> Prior to the digestion, all samples were diluted with Milli-Q water to reach a lipid content of around 2.5 wt%.

Simulated gastric fluid (SGF) was prepared using HCl (37% concentrated, 0.7 mL), NaCl (0.2 g) and pepsin (320 mg) added in 100 mL of Milli-Q water, and then adjusted to pH 1.2. Every diluted sample (15 mL) was mixed with the freshly prepared SGF at a ratio of 1 : 1 (v/v). The mixture was adjusted to pH 2.5 using 1.0 M NaOH and then incubated at 37 °C with continuous agitation at 250 rpm for 120 min.

Simulated intestinal fluid (SIF), containing 1.5 mL of salt solution (110 mg mL $^{-1}$ , CaCl $_2$ ; 13 mg mL $^{-1}$ , NaCl) and 3.5 mL of bile salt extract solution (54 mg mL $^{-1}$  in 5 mM phosphate

buffer, pH 7.0), was added to the gastric phase and readjusted to pH 7.0. A lipase suspension (2.5 mL, 24 mg mL $^{-1}$  in 5 mM phosphate buffer, pH 7.0) was incorporated into the mixture. The mixture was maintained at pH 7.0 by titrating with 1.0 M NaOH to quantify the free fatty acids (FFAs) released from the samples. The whole process was conducted in a 37 °C water bath, and the mixture was incubated with continuous agitation at 250 rpm for 120 min. The hydrolysis of lipids was quantified by calculating the FFA release according to eqn (2):

$$\text{FFAs (\%)} = \frac{V_{\text{NaOH}} \times 1.0 \text{ M} \times M_{\text{Lipid}}}{2 \times W_{\text{Lipid}}} \times 100\% \quad (2)$$

where  $V_{\text{NaOH}}$  is the volume (L) of 1.0 M NaOH used to neutralize the released FFAs in the digestion model.  $M_{\text{Lipid}}$  is the average molecular weight of hemp seed oil (874 g mol $^{-1}$ ).  $W_{\text{Lipid}}$  is the total lipid mass applied in the digestion model.

After the small intestinal phase digestion, the digesta were centrifuged at 10 000g at 4 °C for 60 min to collect the micellar phase. The concentration of CBD in the micellar phase was determined with UPLC as described in section 2.7. The bioaccessibility of CBD after digestion was calculated according to eqn (3):

$$\text{Bioaccessibility (\%)} = \frac{C_{\text{Micellar}}}{C_1} \times 100\% \quad (3)$$

where  $C_{\text{Micellar}}$  is the concentration of CBD in the micellar phase and  $C_1$  is the concentration of CBD encapsulated in digesta.

## 2.10 Statistical analysis

All measurements were carried out more than three times and expressed as mean value  $\pm$  standard deviation. The significance ( $p < 0.05$ ) was analyzed by the analysis of variance (ANOVA) and Duncan's test using IBM SPSS statistical software (version 28.0.1.1, IBM SPSS, USA).

# 3. Results and discussion

## 3.1 Influence of the oleosome membrane on *in vitro* lipid digestion

To understand the differences in the lipid digestion rate of oleosomes in relation to other oil droplets, we compared them to oil droplets stabilised by commonly used emulsifiers, like whey proteins (WPI), phospholipids (PL) and a WPI + PL mixture.<sup>19,20</sup>

Fig. 1A shows the release of FFAs from the four types of emulsions during the small intestinal phase. The release of FFAs of oil droplets stabilized by WPI + PL, WPI and PL followed a typical trend characterized by an initial sharp increase in the released FFA followed by a progressively slower increase. The oil droplets stabilized with only WPI or PL exhibited a slightly faster FFA release rate during the first 70 min compared to the emulsions stabilized with the WPI + PL mixture. This synergy may result from a better coverage of the oil/water interface by the combination of WPI and PL (Fig. 1B). As a



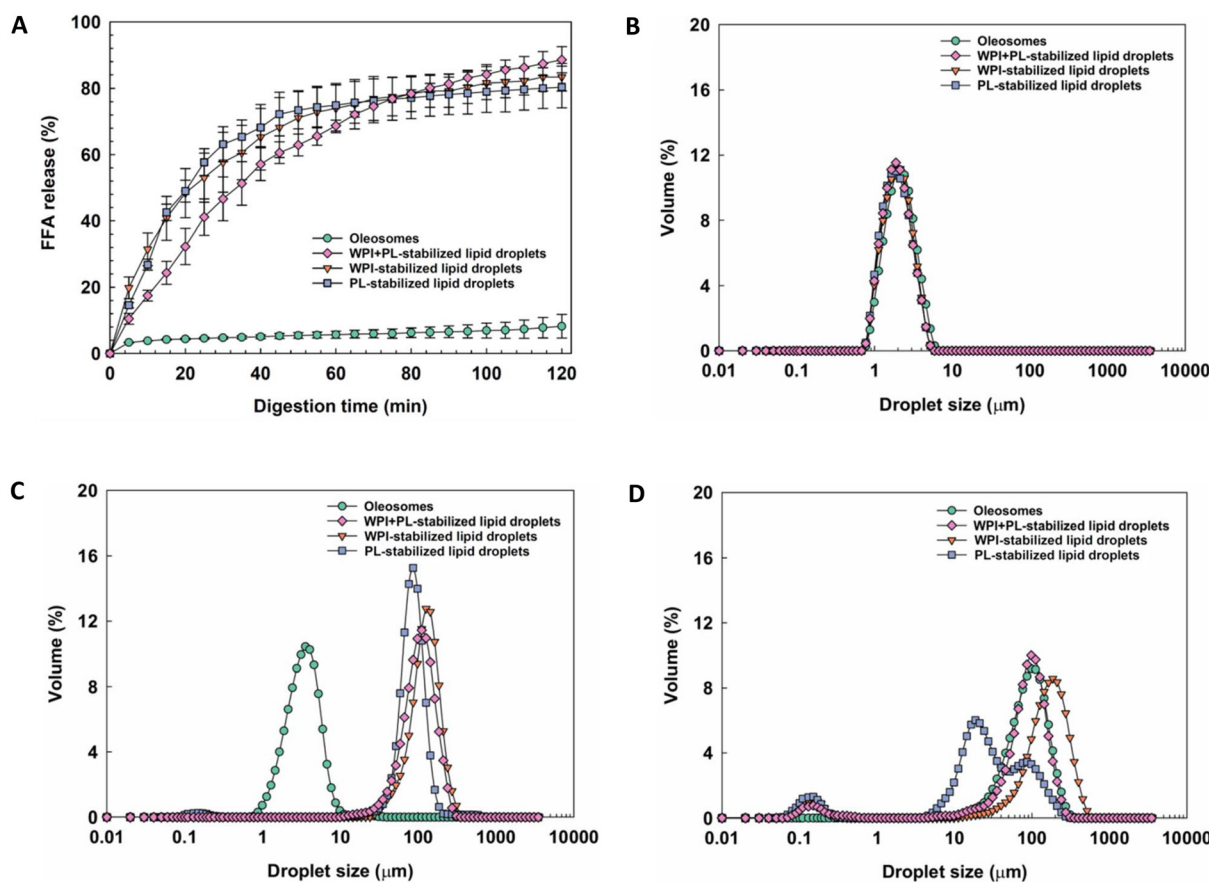


**Fig. 1** Free fatty acid release from oleosomes and emulsions stabilized by WPI + PL, WPI and PL during 2 h of small intestinal phase digestion ( $N \geq 3$ , mean value  $\pm$  standard deviation) (A). Droplet size distribution of oleosomes and emulsions stabilized by WPI + PL, WPI and PL before digestion (B), after the gastric phase (C) and after the small intestinal phase (D). All samples were diluted with Milli-Q water to reach a lipid content of around 2.5 wt% before starting the digestion experiments.

result, the release of FFAs was initially slower. However, after 120 min of *in vitro* small intestinal phase digestion, the WPI + PL-stabilized oil droplets had a similar FFA release to the WPI- or PL-stabilized oil droplets at around 89%, 83% and 80%, respectively. This is significantly higher than that of the oleosomes, which exhibit very slow and continuous release to reach a final value of only 8.21%. It is worth noticing that the observed differences in the FFA release between oleosomes and the WPI, PL, and WPI + PL-stabilized emulsions cannot be explained by differences in the initial size distribution of the emulsion. Indeed, all the emulsions showed a unimodal droplet size distribution with droplet sizes around 2.0  $\mu\text{m}$ , similar to the oleosomes (Fig. 1B). However, we observed differences in the droplet size distributions at the end of the gastric step of the simulated *in vitro* digestion. The droplet sizes of the emulsions increased to 122.4  $\mu\text{m}$  (WPI + PL), 163.7  $\mu\text{m}$  (WPI), and 87.2  $\mu\text{m}$  (PL) after the gastric phase, as shown in Fig. 1C. In contrast, the droplet size of oleosomes was 6.7  $\mu\text{m}$  after the gastric phase. The total surface area of the emulsion at the beginning of the small intestinal phase is known to be one of the most important factors governing lipid hydrolysis *in vitro* and *in vivo*. It has been reported that PL-

stabilized emulsions may resist coalescence during the gastric phase of digestion and present a relatively high total surface with a smaller droplet size at the beginning of the small intestinal phase and, therefore, are digested rapidly. Instead, the proteins in WPI + PL and WPI stabilized emulsions could be hydrolyzed into peptides by pepsin in the gastric phase.<sup>21</sup> This may produce a certain degree of droplet coalescence and facilitate their removal by bile salts in the small intestinal phase, facilitating the exposure of the oil cores to lipase, thus enhancing lipid hydrolysis and the subsequent release of FFAs.<sup>22</sup> This modification of the droplet interface produced differences in the total surface area exposed to lipase in the small intestinal phase by droplet coalescence. At the end of the small intestinal phase, the droplet size of emulsions changed to 112.8  $\mu\text{m}$  (WPI + PL), 182.1  $\mu\text{m}$  (WPI), and 62.5  $\mu\text{m}$  (PL), respectively (Fig. 1D). It has been proposed that the oleosome membrane remains stable due to the structure of the oleosins combined with the presence of the phospholipids providing resistance to gastric digestion, as the hydrophobic domain of the oleosins embedded in the lipid core is less accessible to pepsin, and can maintain some stability of the oleosomes even after partial hydrolysis of the hydrophilic regions.<sup>10</sup> Moreover,

the compact oleosin and phospholipid structures may prevent the adsorption of bile salts and lipase onto the interface. They formed large aggregates of oleosomes which increased to 103.5  $\mu\text{m}$  after the small intestinal phase that further hindered the hydrolysis by reducing the access for lipase<sup>10</sup> and slowed the release of FFAs during the small intestinal phase digestion.<sup>23,24</sup> The substantial lower lipid digestion of the oleosome cannot be explained by a larger droplet size, for instance, as a result of coalescence (and hence a lower surface area for lipase) in the gastric phase as previously reported.<sup>11,25</sup> As displayed in Fig. 1C, the droplet size of the oleosome after the gastric phase was considerably smaller than in the other emulsions. Even though the total surface area of oleosomes at the beginning of the small intestinal phase was the larger than that of artificial emulsions, the FFA release was still the lowest among the tested samples. Differences in the interfacial properties of oleosomes and WPI + PL, WPI and PL-stabilized oil droplets, particularly the hairpin structure of the oleosins on the surface of oleosomes, are therefore more likely attributable to the observed limited digestibility of the oleosomes.

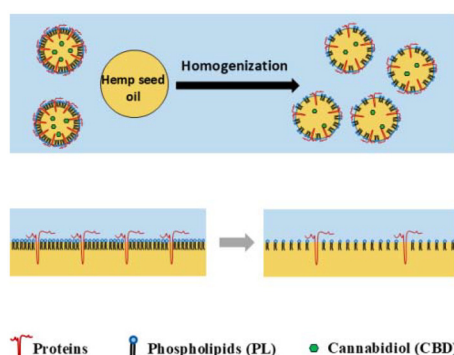


Fig. 2 Schematic representation of the difference in membrane density between oleosomes (bottom left) and oleosomes homogenized with oil (bottom right).

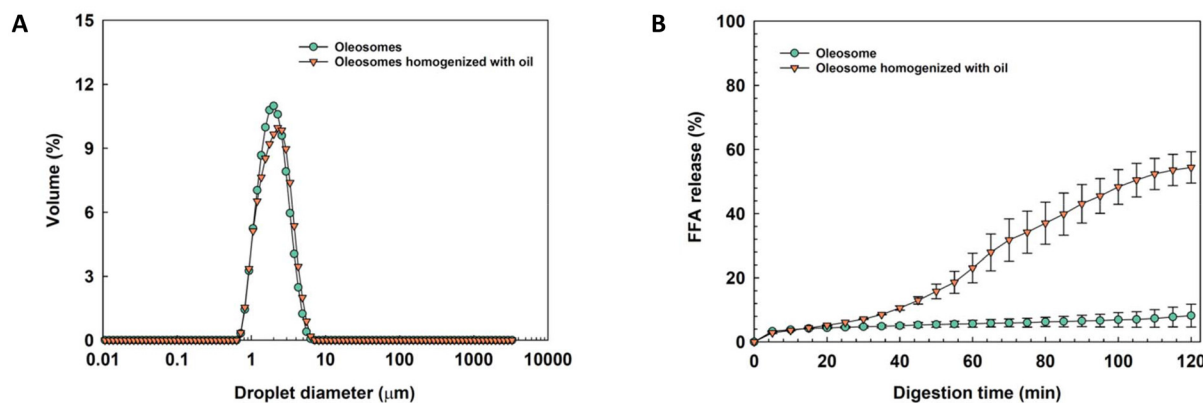
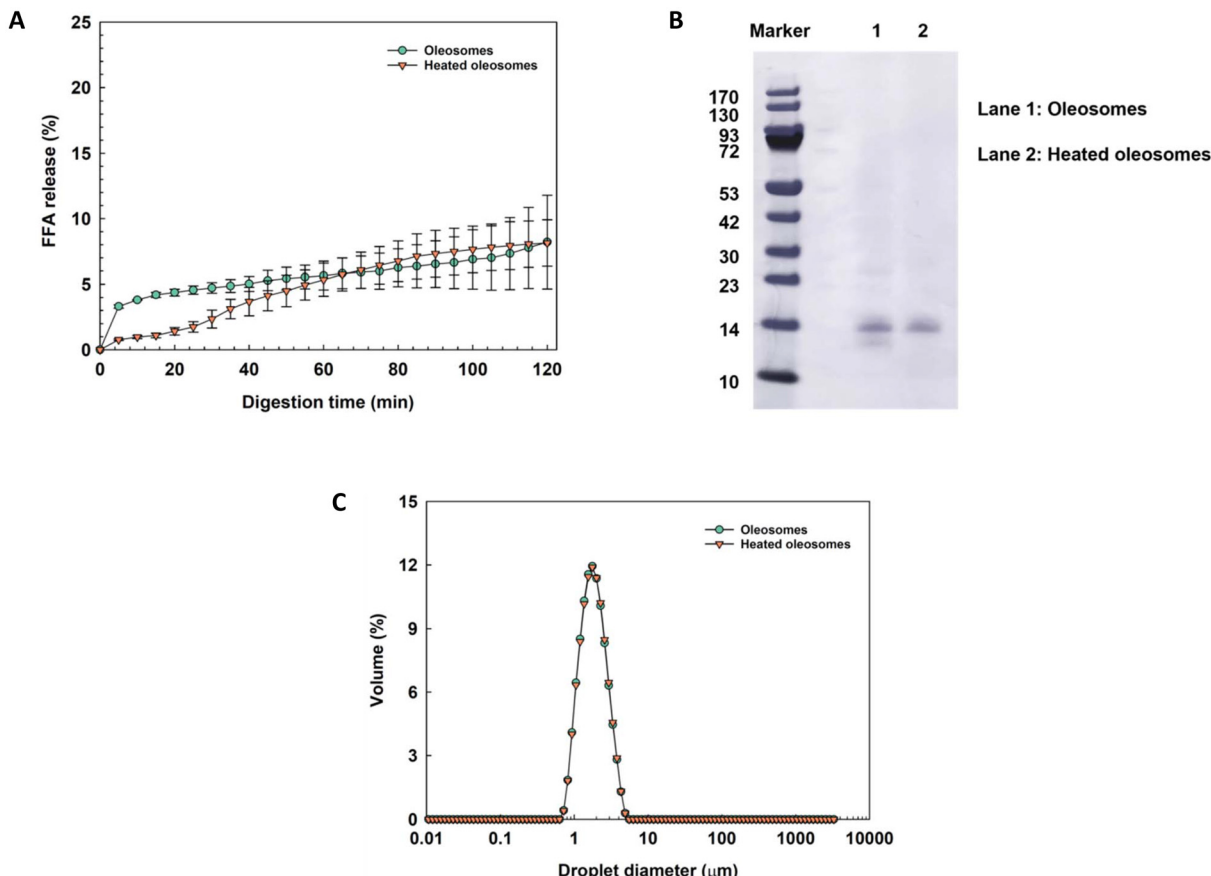


Fig. 3 (A) Droplet size distribution of oleosomes and oleosomes homogenized with oil. (B) Free fatty acid release from oleosomes and oleosomes homogenized with oil during 2 h of small intestinal phase digestion ( $N \geq 3$ , mean value  $\pm$  standard deviation). All samples were diluted with Milli-Q water to reach a lipid content of around 2.5 wt% before starting the digestion experiments.

### 3.2 Influence of the membrane density on *in vitro* digestion

The interfacial properties of oleosomes are characterized by a compact membrane structure comprising proteins and phospholipids and a high membrane density. A previous study estimated that the interface density of rapeseed oleosomes was one phospholipid molecule (PL) per  $\text{nm}^2$ , a far higher phospholipid interfacial density sufficient for stabilization (0.1–0.2 PL per  $\text{nm}^2$ ).<sup>26</sup> Therefore, to further explore the role of the oleosome interfacial properties in the limited digestibility, the membrane density was manipulated by adding additional hemp seed oil to oleosome dispersions (3.75 wt% lipid content), which were then homogenized at the optimal high-pressure to obtain an oleosome dispersion with 7.5 wt% lipid content.<sup>26,27</sup> The resulting homogenized oleosomes had a membrane density approximately half that of the original oleosomes (schematically represented in Fig. 2) but with a droplet size and size distribution (Fig. 3A) comparable to those of the original oleosome dispersion.

Fig. 3B shows that the release of FFAs from the oleosomes with lower membrane density was much higher (55%) than that from native oleosomes (8%) during the small intestinal tract digestion. The droplet sizes of both systems at the beginning of the digestion were similar. Therefore, the difference could be attributed to the different types of access of bile salts and enzymes to the oleosome membrane and the inner triacylglycerols. The available oil surface is increased during homogenization with the additional oil, and the membrane molecules are expected to redistribute on the surface.<sup>26</sup> With the increased total surface areas, the homogenized oleosomes had reduced membrane density and a weakened molecular lateral interactions at the interface which created voids on the droplet surface.<sup>26</sup> The voids facilitate the access of digestive enzymes through the reduced density membrane, increasing the chance of contact with the lipids in oleosomes and enhancing the hydrolysis of the lipids. Interestingly, both systems in Fig. 3B had similar initial FFA release kinetics in the first 20 min, suggesting that the voids on the oleosome interface are rela-



**Fig. 4** (A) Free fatty acid release from native oleosomes and heated oleosomes in an *in vitro* digestion model (mean value  $\pm$  standard deviation). (B) Protein profiles of native oleosomes and heated oleosomes by SDS-PAGE. (C) Droplet size distribution of native oleosomes and heated oleosomes. All samples were diluted with Milli-Q water to reach a lipid content of around 2.5 wt% before starting the digestion experiments.

tively small, and the rate at which the enzymes reach the oleosome TAGs is not too high. After the first 20 min, the lipid hydrolysis at the homogenized oleosomes increased, showing that the lipases had easy access to the oleosome TAGs.

### 3.3 Influence of heat treatment on *in vitro* digestion

Heat treatment is commonly used in food production and processing for a variety of reasons. The natural structure of proteins on the surface of oleosomes might be changed by heating, modifying their interfacial behavior and the stabilization of oleosomes.<sup>13,14</sup> Therefore, oleosomes were heated at 95 °C for 30 min and then subjected to *in vitro* digestion to characterize the influence of the heat treatment on their digestibility.

Fig. 4A shows that both native and heated oleosomes exhibit only very gradual FFA release, reaching only approximately 8% after 120 min of small intestinal phase digestion, with no significant difference between heated and unheated oleosomes. This agrees with a previous study indicating that heating does not enhance the FFA release from oleosomes during *in vitro* digestion, as it depends on the accessibility of the oil-water interface for the lipase, which does not change.<sup>13</sup> However, a previous study reported that roasted hazelnut oleo-

somes exhibited a higher FFA release than raw hazelnut oleosomes.<sup>10</sup> The case may be made that the effect of heating on the interfacial properties, particularly the interaction between protein and their native structures, could vary depending on the severity of the heat treatment, which was quite strong on the roasted hazelnut oil bodies (140 °C, 20 min). In our study, we opted for a milder heating condition of 95 °C for 30 min, which may only impact the interfacial properties of oleosomes from hemp seeds to a limited extent. Interestingly, there was a substantial difference in the kinetics of the FFA release in the first 60 min during the small intestinal phase of digestion. We hypothesize that heat treatment alters the protein structure at the oleosome interface. This alteration may enhance  $\beta$ -folding and induce a random coil in the hydrophilic regions of the interface proteins.<sup>14</sup> These structural changes could render the proteins less susceptible to proteases, which may explain the slower hydrolysis rate during the early phase of digestion. However, after this initial period, there is no significant difference in FFAs released between the heated and unheated oleosomes. The protein composition of the native and heated oleosomes was characterized by SDS-PAGE, as shown in Fig. 4B. The oleosomes were highly purified with negligible amounts of impurities, such as exogenous proteins on the surface. A



main band of around 14 kDa was present and assigned to oleosins on the SDS-PAGE gel.<sup>5</sup> Oleosins remained on the surface of oleosomes and showed no significant changes before and after the heat treatment. It did not appear, as previously reported, that the exogenous protein dissociated from the interface upon heating, which would lead to instability in the heated oleosome and increase the rate of *in vitro* digestion.<sup>13</sup> Instead, the purified oleosomes we obtained maintained good stability even after heating. Moreover, the native and heated oleosomes had similar droplet size and distribution, indicating that oleosomes showed excellent thermal stability without aggregation, flocculation or phase separation during the heating process, as shown in Fig. 4C. Therefore, a relatively mild heat treatment does not change the structure of the oleosins, nor does it change the properties of the oleosomes.

### 3.4 Bioaccessibility of CBD

The bioaccessibility of the encapsulated target compound, *i.e.*, its effective delivery and release in the small intestinal phase digestion, is an important parameter for judging the efficacy of a carrier system.<sup>28</sup> Therefore, the bioaccessibility of CBD of different types of oleosomes was investigated and the results are shown in Fig. 5. The oleosomes homogenized with additional oil showed a much higher CBD bioaccessibility, 42%, compared to the native and heated oleosomes at 7% and 6%, respectively. This implies that reducing the membrane density of oleosomes could effectively increase the bioaccessibility of CBD. Moreover, according to the trends of FFA release, both the oil and the CBD will only be gradually released.

It was reported earlier that oleosome-based carriers had a relatively lower *in vitro* bioaccessibility of CBD compared to emulsions stabilized by regular emulsifiers.<sup>29,30</sup> There is a direct correlation between the bioaccessibility of CBD and the release of the FFAs. A higher FFA release during *in vitro* digestion also results in a higher bioaccessibility of CBD. The phos-

pholipid density of the membrane, plus its stabilization by the oleosins, gives oleosomes a strong resistance to digestion, which leads to a low lipid hydrolysis rate and low bioaccessibility of CBD. Modification of the membrane density by dilution with refined oil provides a simple way to customize CBD bioaccessibility, exceeding the bioaccessibility in pure CBD oil, which was only 1.83% (Fig. 5). The combined stability of the oleosomes against heating and loading with active components, plus their suitability for modification of their properties, show their versatility as delivery vehicles for therapeutics and other bioactive components.

## 4. Conclusions

In this study, the influence of the membrane density of oleosomes on *in vitro* lipid digestion of oleosomes and CBD bioaccessibility was investigated. The hairpin structure of the oleosins that stabilize the oleosomes, plus the dense packing of phospholipids, produced a slow and constant FFA release in the *in vitro* small intestinal model used. Furthermore, the heating of oleosomes did not lead to changes in their digestibility.

The influence of membrane density was demonstrated by 'diluting' oleosomes with additional refined oil, such that the resulting oleosomes only had half the membrane density of the native ones but the same droplet size. The 'diluted' oleosomes with half the membrane density had a significantly higher FFA release (55%) after *in vitro* digestion than the undiluted ones (8%). Thus, the bioaccessibility of CBD can be modulated by manipulation of the membrane density, which highlights the potential of oleosomes as efficient delivery vehicles for functional ingredients.

## Author contributions

Zhaoxiang Ma: conceptualization, methodology, investigation, formal analysis, validation, visualization, data curation, and writing – original draft; Edoardo Capuano: writing – review and editing; Johannes H. Bitter: supervision and writing – review and editing; Remko M. Boom: supervision and writing – review and editing; Constantinos V. Nikiforidis: conceptualization, methodology, supervision, and writing – review and editing.

## Data availability

The authors confirm that the data supporting the findings of this study are available within the article.

## Conflicts of interest

The authors declare that there are no conflicts of interest.

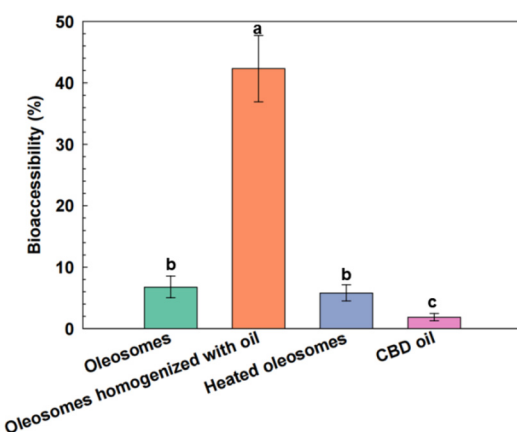


Fig. 5 Bioaccessibility of cannabidiol (CBD) in oleosomes, oleosomes homogenized with oil, heated oleosomes and CBD oil after *in vitro* digestion ( $N \geq 3$ , mean value  $\pm$  standard deviation). All samples had the same CBD and lipid concentrations.



## Acknowledgements

The authors would like to thank Botaneco Inc. for providing financial support.

## References

- 1 S. U. Rawal and M. M. Patel, in *Lipid nanocarriers for drug targeting*, Elsevier, 2018, pp. 49–138.
- 2 P. Ghasemiyeh and S. Mohammadi-Samani, Solid lipid nanoparticles and nanostructured lipid carriers as novel drug delivery systems: Applications, advantages and disadvantages, *Res. Pharm. Sci.*, 2018, **13**, 288–303.
- 3 B. K. Panigrahi and A. K. Nayak, Carbon nanotubes: An emerging drug delivery carrier in cancer therapeutics, *Curr. Drug Delivery*, 2020, **17**, 558–576.
- 4 L. Sercombe, T. Veerati, F. Moheimani, S. Y. Wu, A. K. Sood and S. Hua, Advances and challenges of liposome assisted drug delivery, *Front. Pharmacol.*, 2015, **6**, 163819.
- 5 Z. Ma, J. H. Bitter, R. M. Boom and C. V. Nikiforidis, Thermal treatment improves the physical stability of hemp seed oleosomes during storage, *LWT-Food Sci. Technol.*, 2023, 115551.
- 6 C. V. Nikiforidis, Structure and functions of oleosomes (oil bodies), *Adv. Colloid Interface Sci.*, 2019, 102039.
- 7 J. Yang, L. Plankenstein, A. de Groot, M. Hennebelle, L. M. C. Sagis and C. V. Nikiforidis, The role of oleosins and phosphatidylcholines on the membrane mechanics of oleosomes, *J. Colloid Interface Sci.*, 2025, **678**, 1001–1011.
- 8 Z. Ma, J. H. Bitter, R. M. Boom and C. V. Nikiforidis, Encapsulation of cannabidiol in hemp seed oleosomes, *Food Res. Int.*, 2024, **195**, 114948.
- 9 U. S. Vardar, J. H. Bitter and C. V. Nikiforidis, The mechanism of encapsulating curcumin into oleosomes (lipid droplets), *Colloids Surf., B*, 2024, **236**, 113819.
- 10 E. Capuano, N. Pellegrini, E. Ntone and C. V. Nikiforidis, In vitro lipid digestion in raw and roasted hazelnut particles and oil bodies, *Food Funct.*, 2018, **9**, 2508–2516.
- 11 Y. Sun, M. Zhong, L. Wu, Q. Wang, Y. Li and B. Qi, Loading natural emulsions with nutraceuticals by ultrasonication: Formation and digestion properties of curcumin-loaded soybean oil bodies, *Food Hydrocolloids*, 2022, **124**, 107292.
- 12 J. B. Keogh, T. J. Wooster, M. Golding, L. Day, B. Otto and P. M. Clifton, Slowly and rapidly digested fat emulsions are equally satiating but their triglycerides are differentially absorbed and metabolized in humans, *J. Nutr.*, 2011, **141**, 809–815.
- 13 J. Ding, J. Wen, J. Wang, R. Tian, L. Yu, L. Jiang, Y. Zhang and X. Sui, The physicochemical properties and gastrointestinal fate of oleosomes from non-heated and heated soymilk, *Food Hydrocolloids*, 2020, **100**, 105418.
- 14 J. Ding, Z. J. Xu, B. K. Qi, Z. Z. Liu, L. L. Yu, Z. Yan, L. Z. Jiang and X. N. Sui, Thermally treated soya bean oleosomes: The changes in their stability and associated proteins, *Int. J. Food Sci. Technol.*, 2020, **55**, 229–238.
- 15 S. Pisanti, A. M. Malfitano, E. Ciaglia, A. Lamberti, R. Ranieri, G. Cuomo, M. Abate, G. Faggiana, M. C. Proto and D. Fiore, Cannabidiol: State of the art and new challenges for therapeutic applications, *Pharmacol. Ther.*, 2017, **175**, 133–150.
- 16 A. Fraguas-Sánchez, A. Fernández-Carballido, C. M.-S. Sofware and A. Torres-Suárez, Stability characteristics of cannabidiol for the design of pharmacological, biochemical and pharmaceutical studies, *J. Chromatogr. B: Biomed. Sci. Appl.*, 2020, 122188.
- 17 C. Lopez, B. Novales, H. Rabesona, M. Weber, T. Chardot and M. Anton, Deciphering the properties of hemp seed oil bodies for food applications: Lipid composition, microstructure, surface properties and physical stability, *Food Res. Int.*, 2021, **150**, 110759.
- 18 Z. Ma, Y. Zhao, N. Khalid, G. Shu, M. A. Neves, I. Kobayashi and M. Nakajima, Comparative study of oil-in-water emulsions encapsulating fucoxanthin formulated by microchannel emulsification and high-pressure homogenization, *Food Hydrocolloids*, 2020, 105977.
- 19 L. Plankenstein, J. Yang, J. H. Bitter, J.-P. Vincken, M. Hennebelle and C. V. Nikiforidis, High yield extraction of oleosins, the proteins that plants developed to stabilize oil droplets, *Food Hydrocolloids*, 2023, **137**, 108419.
- 20 Z. Ma, N. Khalid, G. Shu, Y. Zhao, I. Kobayashi, M. A. Neves, A. Tuwo and M. Nakajima, Fucoxanthin-loaded oil-in-water emulsion-based delivery systems: Effects of natural emulsifiers on the formulation, stability, and bioaccessibility, *ACS Omega*, 2019, **4**, 10502–10509.
- 21 M. Golding, T. J. Wooster, L. Day, M. Xu, L. Lundin, J. Keogh and P. Clifton, Impact of gastric structuring on the lipolysis of emulsified lipids, *Soft Matter*, 2011, **7**, 3513–3523.
- 22 H. Singh, A. Ye and D. Horne, Structuring food emulsions in the gastrointestinal tract to modify lipid digestion, *Prog. Lipid Res.*, 2009, **48**, 92–100.
- 23 S. Gallier and H. Singh, Behavior of almond oil bodies during in vitro gastric and intestinal digestion, *Food Funct.*, 2012, **3**, 547–555.
- 24 R. S. Li, C. F. Pu, Y. Sun, Q. J. Sun and W. T. Tang, Interaction between soybean oleosome-associated proteins and phospholipid bilayer and its influence on environmental stability of luteolin-loaded liposomes, *Food Hydrocolloids*, 2022, **130**, 107721.
- 25 J. Zhu, H. Wang, L. Miao, N. Chen, Q. Zhang, Z. Wang, F. Xie, B. Qi and L. Jiang, Curcumin-loaded oil body emulsions prepared by an ultrasonic and pH-driven method: Fundamental properties, stability, and digestion characteristics, *Ultrason. Sonochem.*, 2023, **101**, 106711.
- 26 E. Ntone, B. Rosenbaum, S. Sridharan, S. B. Willems, O. A. Moultsos, T. J. Vlugt, M. B. Meinders, L. M. Sagis, J. H. Bitter and C. V. Nikiforidis, The dilatable membrane of oleosomes (lipid droplets) allows their in vitro resizing and triggered release of lipids, *Soft Matter*, 2023, **19**, 6355–6367.
- 27 E. Ntone, J. Yang, M. B. Meinders, J. H. Bitter, L. M. Sagis and C. V. Nikiforidis, The emulsifying ability of oleosomes



and their interfacial molecules, *Colloids Surf. B*, 2023, **229**, 113476.

28 C. Dima, E. Assadpour, S. Dima and S. M. Jafari, Bioavailability and bioaccessibility of food bioactive compounds; Overview and assessment by in vitro methods, *Compr. Rev. Food Sci. Food Saf.*, 2020, **19**, 2862–2884.

29 H. Zheng, B. Chen and J. Rao, Nutraceutical potential of industrial hemp (*Cannabis sativa* L.) extracts: Physicochemical stability and bioaccessibility of cannabidiol (CBD) nanoemulsions, *Food Funct.*, 2022, **13**, 4502–4512.

30 C. Wang, C. Dong, Y. Lu, K. Freeman, C. Wang and M. Guo, Digestion behavior, in vitro and in vivo bioavailability of cannabidiol in emulsions stabilized by whey protein-maltodextrin conjugate: Impact of carrier oil, *Colloids Surf. B*, 2023, **223**, 113154.